

**Spatial spectra of scalp EEG and EMG from awake humans**

Walter J Freeman  
Department of Molecular & Cell Biology  
University of California, LSA 142, MC 3200  
Berkeley CA 94720 USA  
wfreeman@socrates.berkeley.edu

Mark D Holmes  
EEG & Clinical Neurophysiology Laboratory  
325 Ninth Ave, Harborview Medical Center  
Box 359722, Seattle, WA 98104  
mdholmes@u.washington.edu

Brian C Burke  
Department of Molecular & Cell Biology  
University of California, LSA 142, MC 3200  
Berkeley CA 94720 USA  
burkeb@uclink.berkeley.edu

Sampsa Vanhatalo  
EEG & Clinical Neurophysiology Laboratory  
325 Ninth Ave, Harborview Medical Center  
Box 359722, Seattle, WA 98104  
sampsav@u.washington.edu

Clin. Neurophysiol. 114 (6): 1055-5060, 2003

**Running title:** Spectra of scalp EEG and EMG

**Key words:** EEG scalp, EMG scalp, Hilbert transform EEG/EMG, power spectral density EEG/EMG, spatial spectrum EEG/EMG

**Acknowledgments**

Data were from the EEG Clinic, Harborview Hospital, Seattle WA. The linear electrode array was constructed there by Anthony Bell in accordance with a Berkeley design. Analyses were done in the Division of Neurobiology at Berkeley. Discussions with Ceon Ramon and Linda Rogers are gratefully acknowledged. Partial support was provided through a grant NCC 2-1244 from NASA and a grant EIA-0130352 from NSF.

## Abstract

**Objectives:** Evaluate spectral scaling properties of scalp electroencephalogram (EEG) and electromyogram (EMG), optimal spacing of electrodes, and strategies for mitigating EMG.

**Methods:** EEG was recorded referentially from 9 subjects with a 64 channel linear array (electrodes 3 mm apart) placed parasagittally or transversely on forehead or occiput, at rest with eyes open or closed, or with deliberate EMG. Temporal ( $PSD_t$ ) and spatial ( $PSD_x$ ) power spectral densities were calculated with 1-dimensional fast Fourier transform (FFT) for comparison with earlier analyses of intracranial EEG.

**Results:** Scaling of  $PSD_t$  from scalp resembled that from pia: near-linear decrease in log power with increasing log frequency ( $1/f^\alpha$ ). Scalp  $PSD_x$  decreased nonlinearly and more rapidly than  $PSD_x$  from pia. Peaks in  $PSD_t$  (especially 4-12 Hz) and  $PSD_x$  (especially 0.1-0.4 cycles/cm) revealed departures from  $1/f^\alpha$ . EMG power in  $PSD_t$  was more 'white' than  $1/f^\alpha$ .

**Conclusions:** Smearing by dura-skull-scalp distorts  $PSD_x$  more than  $PSD_t$  of scalp EEG from  $1/f^\alpha$  scaling at the pia. Spatial spectral peaks suggest that optimal scalp electrode spacing might be  $\sim 1$  cm to capture nonlocal EEG components having the texture of gyri. Mitigation of EMG by filtering is unsatisfactory. A criterion for measuring EMG may support biofeedback for training subjects to reduce their EMG.

**Significance:** High-density recording and log-log spectral display of EEG provide a foundation for holist studies of global human brain function, as an alternative to network approaches that decompose EEG into localized, modular signals for correlation and coherence.

## Introduction

The ready availability of large banks of commercial amplifiers has facilitated the detailed imaging of brain electrical activity with high density electrode arrays. A common approach for interpretation and spatial analysis is to assume that cortex is composed of a mosaic of quasi-autonomous areas (Bressler, Coppola and Nakamura, 1993; Bressler, 1996; Calvin, 1996; Taylor, 1997; Varela et al., 2001). Each area transmits a signal to one or more other areas in a network, and its signal may appear in the scalp EEG, where it overlaps with other signals both spatially and temporally by volume conduction. If a signal can be extracted from an area and be associated with a particular behavior, then the special contribution of that area to the behavior might be explained. One technique for signal extraction is deconvolution by using the Laplacian operator (Gevins et al., 1997; Srinivasan, Nunez and Silberstein, 1998) or an equivalent (Freeman, 1980). Another technique is to decompose EEG from multiple electrodes by temporal filters, wavelets, or the FFT into specific frequencies in search of high correlation and coherence, which might reflect episodic transmission or cooperation between pairs or networks of areas in conjunction with behavior. However, the use of Fourier decomposition is ill-suited for the nonlinearities and broad-spectra of many signals in brains (Lachaux et al. 1999; Mingzhou et al 2000; Nunez et al. 1997; Srinivasan et al 1998), owing to the assumption of linearity. Also, the pair-wise treatment of component relations by the FFT does not give a strong base for addressing mechanisms of global integration across continuous distributions of power in space and frequency.

A holist approach pursued here as an alternative to network approaches is to assume that the forebrain is a highly unstable organ that maintains itself in a global state of self-organized criticality (Bak, Tang and Wiesenfeld, 1987). Covariance emerges from local interactions and expands over long distances in time and space. The activity patterns at all levels show

power-law scaling behavior. Bak et al. (1987) proposed that "SOC" enables a large and complex system to change rapidly in response to unpredictably fluctuating inputs, such as the brain engaged with its environment. Power-law scaling in systems at SOC is suggested by a linear decrease in log power with increasing log frequency ( $1/f^\beta$ ). This form is found on epileptic EEG on calculating both temporal power spectral density ( $PSD_t$ ) and spatial power spectral density ( $PSD_x$ ) (Freeman et al., 2000). The scaling properties of criticality are such that spatially coherent cortical activity patterns may coexist for epochs ranging in duration from a few ms to several seconds, and with diameters ranging from a few mm to an entire hemisphere, building from columns to gyri to lobes. However, in practice the estimation of the critical exponent,  $\beta$ , is uncertain. Spectral forms are distorted by sharp spectral peaks from narrow band oscillations, usually in the classical ranges of alpha, theta, and "40 Hz" at irregular times for varying durations (Linkenkaer-Hansen, 2001).

The scaling behavior of temporal patterns has been well studied (Ingber, 1995), particularly in the alpha and beta ranges (Nunez et al., 1997; Linkenkaer-Hansen et al., 2001). An aim in the present study was to study scaling in scalp EEG in the spatial frequency domain, in order to develop an experimental data base with which to explore SOC in normal human subjects. Gamma oscillations were especially targeted, because they have been found in local brain areas having the privileged input and output connections of sensory and motor cortices (Singer and Gray, 1995; Dumenko, 2000; Freeman, 2000). Gamma has also been found over large scalp areas in association with diverse cognitive behaviors, by means of band pass filtering (Sheer, 1976; Haig et al. 2000) or wavelet decomposition (Tallon-Baudry et al., 1996, 1998). If SOC holds, these temporal properties could be expected to change abruptly both locally and globally several times a second during normal behavior.

Gamma activity might also have spatial structures varying widely in size and duration, as it does in animals (Freeman and Barrie, 2000; Freeman, 2003). The spatial scaling of brain activity patterns is much less well known. Normative data are needed to describe its properties over a wide range of spatial frequencies. Low frequencies should correspond to the sizes of areas that may be linked in the production of behavior, while higher frequencies may reflect the textures of the patterns within the areas. An essential tool with which to explore these properties with digital signal processing is spatial spectral analysis (Gonzalez and Wintz, 1977; Barlow, 1993). For the one-dimensional (1-D) case used here with a linear array, this procedure is mathematically identical to applying the one-dimensional fast Fourier transform (1-D FFT) to a time series.

The choice of electrode interval is equivalent to the selection of a digitizing rate. For an unknown signal the sampling rate must be faster than all suspected frequency components of the signal to avoid aliasing, and the electrodes must be close enough to capture the texture of the patterns. Oversampling wastes resources by redundancy. In the time domain it limits the duration of a recording epoch, and in the space domain it limits the size of the window onto an area for inspection. An analysis of epileptical EEG (Freeman et al., 2000) was done with a linear 1x64 electrode array by oversampling using .05 cm spacing. The array length (3.15 cm) was short enough for placement by a neurosurgeon on a typical human gyrus (3-5 cm) without bridging a sulcus. The optimal electrode spacing proved to be .125 cm. An optimal spacing for scalp EEG (Hall, 1979; Spitzer et al., 1980) was determined theoretically and experimentally by Srinivasan, Tucker and Murias (1998) as about 3 cm. Experimental evaluation was proposed in the present project by oversampling with a 1-D electrode array of .3 cm spacing. It was short enough (18.9 cm) to fit onto the head for scalp recording. Linear spacing at 3 cm would give an array 189 cm long that might wrap four times around the head.

A note is required on what is meant by the "texture" of spatial patterns of EEG. Studies with 8x8 array recordings in animals (Freeman 2000) revealed spatial patterns in the gamma range, in which the wave form of the oscillation, no matter how irregular or non-periodic, was the same over the array. The similarity was measured by the % variance incorporated in the 1st component of PCA (typically >90%). By spatial extrapolation (Freeman and Baird, 1987; Freeman and Barrie, 2000) the area of coherence was shown to extend well beyond the array window. The common wave form defined the size and location of an area. Within the area the amplitude and phase of the wave form varied with location of the individual electrodes in the array. These variations formed the 'textures' of patterns. When measured as the root mean square (rms) amplitude of each signal from an 8x8 array, each pattern was described as a point in 64-space. A large number of spatial amplitude modulation (AM) patterns was collected from animals trained to discriminate conditioned stimuli. The AM patterns formed clusters of points in 64-space. A Euclidean distance measure served to assign individual patterns to the class of conditioned stimuli to which they belonged (Freeman, 2000). As for texture, the goodness of classification of the amplitude patterns depended on the number of electrodes within a coherent domain, not on their specific locations. The information that served for spatial pattern classification with respect to behavior was nonlocal, having the appearance of interference patterns. Spatial localization of components by deconvolution was unnecessary because it added no new information, and it could have been noncontributory, if smoothing were first used to compensate for the high pass filter effects of spatial deconvolution.

Conflicting requirements must be satisfied for studies of textures. The electrodes should be sufficiently close together to keep as many of them as possible within an area with a common wave form. They should be sufficiently widely spaced for each electrode to yield a significant fraction of independent information. Yet they should still be within the area of spatial coherence.. A compromise is usually necessary in the face of a limited number of

channels available, as well as uncertainty about the sizes of such areas and the spatial and temporal frequency ranges of shared activity. Owing to SOC there is the possibility that measurements of the size and texture of coexisting cooperative domains may vary with the size and interelectrode intervals of the electrode arrays. Treatment of these problems in understanding textures requires spectral analysis. The present study was undertaken to extend textural analysis to EEG recorded from the scalp of normal volunteers. Measurements of intentional EMG were included, because EMG may be confused with gamma activity, and criteria are needed with which to detect liminal or occult EMG.

## Methods

The curvilinear electrode array was made using gold-plated connector pins threaded into a band of embroidery fabric with interstices at 3 mm intervals. The scalp was cleaned and dried, and the array was bound firmly onto the forehead across the midline just below the frontal hairline, paracentrally along the part line, or across the occiput. Recordings were monopolar with respect to a reference electrode on the vertex for frontal and occipital recording and the contralateral mastoid for paracentral recording, approximately equidistant from the array electrodes. The ground was located on the contralateral mastoid for frontal and paracentral recording, and on the frontal midline (AFz) for occipital recording. The EEG were amplified with a Nicolet (BMSI 5000) system having a fixed gain of 1628 and analog filters set at 0.5 Hz high pass and 120 Hz low pass. Possible DC offsets of the RC amplifier outputs were removed off-line by subtracting the channel means of each entire recording set. The ADC gave 12 bits with the least significant bit of 0.9 microvolts and a maximal range 4096 bits. Data were digitized at 420 Hz and down-sampled to 200 Hz, with distortion by aliasing likely from 80 to 120 Hz.

Subjects were five male and four female adult volunteers, who were asked to sit in the dark quietly and relax their muscles, first with eyes closed and then with eyes open. A clean record lasting 1 to 4 minutes was selected for off-line editing for each subject and condition: eyes closed, open, and periods of low level EMG activity resembling gamma activity, induced by the subjects with sustained isometric lifting of the forehead or ears. The data were collected in the EEG Clinic of Harborview Hospital, University of Washington, Seattle, and were sent by ftp without identifying markers of personal information to the University of California at Berkeley for analysis. The data collection and management were governed by protocols approved by Institutional Review Boards in both institutions.

For convenience the data for each subject and condition were blocked into matrices of 5,000 data points (25 s). After initial exploration by varying the window duration from 100 to 5,000 data points, a standard duration of 1,000 data points (5 s) was adopted. Temporal  $PSD_t$  were calculated with the 1-D FFT for every channel after applying a Hanning window. The 64  $PSD_t$  were averaged and transformed for display in log-log coordinates. Spatial  $PSD_x$  were calculated by embedding the 64 digitized values at each time step in 32 zeroes on each end, applying a Hanning window and the 1-D FFT, averaging over the 1,000 spectra for each epoch, and transforming to log-log coordinates. The appearance of the  $1/f^\alpha$  form in  $PSD_t$  was usually distorted by local deficits or concentrations of power especially in the low frequency range. The exponent  $\alpha$  was visually determined by drawing a line through the linear segments of the PSD, since linear regression was unreliable.

Most of the data processing was performed with MATLAB software, including convolution in the time domain for temporal filtering with FIR filters estimated using the Parks-McClellan algorithm in MATLAB of order 200. The transition band width was 4 Hz, except in the cases of narrow adjacent temporal filters, where the transition band width was 1 Hz. Special purpose software was developed for spatial filtering (Freeman and Baird, 1987) in the spatial frequency domain by use of the 1-D FFT transform to get the  $PSD_x$ , multiplication with an exponential filter, and use of the inverse transform of the real and imaginary parts of the spectrum to get the filtered spatial patterns for analysis of temporal spectral pass bands (Freeman, 2000). For low pass filters the factor for attenuation,  $A(f_x)$ , ranged between 0 and 1 with increasing frequency,  $f_x$ , by

$$A(f_x) = \exp \{-0.347 [(f_x) / f_0]^n\}, \quad (1)$$

where  $f_0$  was the cut-off frequency,  $n = 2$  for low pass filters, and  $n = -6$  for high pass filters. The effect on the  $PSD_x$  of padding with zeroes was evaluated with standard padding

giving twice the data length (128 bins) and then repeating the 1-D FFT first without padding, giving a length of 64 bins, and then with embedding at twice the standard length (256 bins). The standard embedding gave smoother curves with better spatial frequency resolution than did no padding. Longer embedding merely extended the low frequency ends of the spectra and enhanced a ripple at the upper ends without adding information.

## Results

### 1. Comparison of EEG from occipital, paracentral and frontal sites

To illustrate the recording arrangement a normal brain was obtained from a teaching collection. A montage was constructed of photographs taken from views perpendicular to the curved surface [Figure 1, A]. The radius of the brain was 7.5 cm, and the estimated thickness of the skull and scalp was 1.5 cm. The gyri appeared as light areas, and the outer aspects of the sulci appeared as dark curves, indicating the indentations in the wrinkled surface of the cortex. The circumference of the scalp of the nine subjects varied between 56 and 59 cm, giving an approximate radius of 9 cm for the head. The surface view of the cortex was up-scaled to the area of the scalp. The montage was digitized at a grain of 0.1 cm, and the two-dimensional FFT was used to calculate the spatial spectrum of the cortical surface [Figure 1, B]. The basic form of the spatial spectrum was  $1/f^\alpha$ , where  $\alpha = -1.7$ , with a broad peak in the range of 0.1 to 0.5 c/cm, corresponding to the typical width (1 cm) and length (3-5 cm) of human gyri. Superimposed rows of dots on the photographic montage indicated the length, spacing, and the three locations of the curvilinear array of recording electrodes.

Recording with a linear array gave the kind of signals shown in Figure 2 from a subject at rest with eyes closed for successive placements over the occipital, paracentral and frontal scalp areas. The 8 signals were from 8 adjacent electrodes. Comparisons between sites showed the well-known gradient of alpha amplitude from back to front, with inconsistent differences in power in other bands. Maximal theta activity was found in the paracentral EEG. The temporal power spectral densities ( $PSD_t$ ) were normalized for total power, averaged, and converted for display in log-log coordinates (Figure 3, A, where the spectral ranges adopted in this study are indicated). The same spectra are separated in frame B.

All 9 subjects had  $PSD_t$  with a nearly linear  $1/f^2$  relation in at least one record, usually frontal. All had alpha peaks in other records with a frequency averaging  $9.6 \pm 1.5$  Hz (Coefficient of Variation = 13%), constituting a clear departure from  $1/f^2$ . Theta peaks averaging  $4.7 \pm .65$  Hz (CV = 14%) were most common with paracentral placements. Three subjects had a spectral spike in the gamma range averaging  $40 \pm 2.1$  Hz (CV = 5%). Activity above 80 Hz was not considered further owing to the low digitizing rate and the possibility of aliasing. Estimates of the slopes of  $PSD_t$  were  $\beta = -1.78 \pm .25$  (SE) for frontal and  $\beta = -1.19 \pm .10$  for occipital. Paracentral estimates were unreliable, owing to the spectral peaks and also to the likelihood of occult EMG, as described in the next section. For comparison the slopes of intracranial  $PSD_t$  were  $\beta = -2.32 \pm .27$  (SE) and of intracranial  $PSD_x$   $\beta = -1.97 \pm .14$  (Freeman et al., 2000).

Examples of  $PSD_x$  from the occipital cortex of the 9 subjects at rest with eyes closed are shown in frames C and D. Unlike the  $PSD_x$  from epipial recording (Freeman et al., 2000) the  $PSD_x$  from scalp EEG did not conform to the linear  $1/f^2$  relation. Power fell rapidly in the low spatial frequency range (wave length  $>10$  cm/cycle, "area") and more slowly through the middle range ("texture") to a plateau in the high range ( $<2.5$  cm/cycle, "noise"). The range labeled "area" had frequencies ( $<.1$  cycles/cm) and wave lengths ( $>10$  cm/cycle) corresponding to lobes. The range of "noise" had frequencies ( $>.4$  cycles/cm) and wave lengths (2.5 cm/cycle) in which few sustained peaks were found across temporal bands. The term "texture" was applied to the middle range (half-wave lengths of 1.25 to 5 cm, lying within in the range of the widths and lengths of gyri) in order to focus attention on that part of the spatial spectrum that might (or might not) yield significant new information.

##### Figures 1 to 3 near here #####

The statistical significance of differences at each frequency on Fourier decomposition was evaluated by t-test between array locations for four pooled subjects (Figure 4). The test confirmed the well-known dominance of alpha in occipital over frontal sites but little else besides prominence of frontal delta in the  $PSD_t$ . It indicated no frequency-specific differences in the  $PSD_x$ .

##### Figure 4 near here #####

An alternative analysis led to the discovery of two other systematic departures from the  $1/f$  spectral pattern. A detailed inspection of the irregularities in the middle range of the spatial spectrum was undertaken by examining the relations between the temporal and spatial spectra by a method of band pass decomposition. Each of the 64 signals in a 5 s epoch (1,000 samples/channel from the curvilinear array) was filtered in a narrow temporal band of fixed width. The lowest band was low pass only. The pass band was stepped across the temporal spectrum without gaps or overlaps. For each band the spatial spectrum was taken of the 64 values at every time step that had been included in the temporal signal. The average  $PSD_x$  was calculated from the 1,000 samples in each band and displayed in compressed form. Results were evaluated for band widths of 10, 7, 4 and 2 Hz. The smallest band width gave the clearest peaks in the middle range of the  $PSD_x$ , so the procedure was applied with the 2 Hz width to EEG from the three locations in all subjects.

Representative results (Figure 5) show the  $PSD_x$  from 2 subjects (eyes closed) across the temporal spectrum for upper bound of the bands ranging from 4 to 56 Hz. Maximal power was at low spatial frequency (long wave lengths) in all subjects (shown right to left with increasing temporal frequency in order to display the decrease in log power). Looking at the far right in the low  $PSD_x$  range and in the alpha (7-12 Hz) and theta (3-7 Hz) temporal bands, an excess of power was clearly visible on the ordinates. When such an excess

was found in either or both theta and alpha, along with the companion peak in the  $PSD_t$ , a peak was also found in the middle range of the  $PSD_x$  (.1 to .4 cycles/cm, wave length 2.4 to 10 cm). The peak (as shown by the arrows) appeared across the whole temporal spectrum, often without attenuation with increasing  $PSD_t$ . This spectral pattern was the second clear departure from  $1/f^2$ . It was characteristic of a temporal spike in the EEG that repeated at the theta or alpha rate, and that had a nonlocal, broadly distributed spatial texture.

##### Figure 5 near here #####

The display of temporal spectral bands was complemented by calculating spatial bands at logarithmically scaled intervals across the spatial spectrum (Figure 6). A comparison was made between eyes closed with alpha and eyes open with theta. The test in this and other subjects showed that the alpha and theta peaks often but not invariably extended across the spatial spectrum. The  $PSD_x$  peaks in the middle range were usually at the limit of resolution. This second pattern of departure from  $1/f^2$  was found in 7 subjects in the paracentral area, in subjects 6 in the occipital area, and in one in the frontal area.

##### Figure 6 near here #####

In 3 subjects a small  $PSD_t$  peak was found at or near 40 Hz in the gamma range. Excess power appeared in the  $PSD_x$  only in the low range. There was no accompanying peak in the middle  $PSD_x$  range. The high concentration of power below .04 cycles/cm, indicated 40 Hz coherence over the entire array with a narrow CV. The combination of a narrow temporal peak in  $PSD_t$  associated with a low frequency spatial peak, maximal at .04 cycles/cm (long wave length) in  $PSD_x$ , was also found in 6 subjects with excess power in the beta range (Figure 6). This third spectral departure from  $1/f^2$  was characteristic of wide

area coherence of narrow band oscillation in the beta and gamma ranges, as already well documented in scalp EEG (see Introduction).

## 2. Modifications of EEG spectra on deliberately adding EMG

Characterization of the spectral properties of EMG was undertaken to distinguish it from EEG. In contrast to epipial and intracerebral signals, the scalp signals were readily subject to contamination with muscle potentials that mimicked or masked components of the signals and might have been occult. Subjects were asked to tense their scalp muscles either by wrinkling their foreheads or straining their neck or ears in isometric contraction without movement, while keeping their eyes closed. A 2- to 3-fold increment in EEG amplitude referential to the vertex was sought, having sustained high frequency oscillations resembling beta and gamma activity but no movement artifacts. Five subjects succeeded in meeting these criteria. Two types of EMG were studied, one from fasciculation and the other more regular in appearance, as shown in Figure 7, where the representative samples in the left and right frames were from the same consecutive channels at 3 mm intervals. For comparison with an intentional act that did not involve the scalp muscles but also reduced alpha, the subjects were also asked to open their eyes and hold still in the dark.

##### Figure 7 near here #####

$PSD_t$  were calculated from each channel in 5 s epochs with and without acceptable EMG and averaged for each subject, array location, and condition.  $PSD_x$  were calculated at each of the 1,000 time points and averaged. For comparison across subject and condition each data set was normalized to zero mean and unit standard deviation. The group mean spectra over the same four subjects are shown in Figure 8 as in Figure 4, with pooling of spectra from the 3 locations. The  $PSD_t$  of the EEG signals gave  $1/f^2$  spectra, usually with

peaks in the alpha and beta ranges and uncommonly at 40 Hz. With EMG onset the alpha peaks usually disappeared. The average power increased over the spectra above and below alpha. Comparison by t-test of the temporal  $PSD_t$  (B) confirmed only the difference accruing from the disappearance of alpha accompanying the effort to control the EMG, and then only at a single frequency in the alpha range. The most significant difference with EMG onset was not revealed by the point-wise t-test at specific frequencies, that the EEG + EMG spectra of both types (summarized in the red curves) departed strongly from  $1/f^2$ . The departure showed that EMG potentials were closer to white noise than to a power-law relation.

##### Figure 8 near here #####

In contrast, there was marked difference in relative power between the  $PSD_x$  in EEG and EEG + EMG compared by t-test with eyes open EEG (Figure 7, D), calling attention to the spatial frequencies in the middle range of .1 to .4 cycles/mm. However, the more salient difference was an increase in the power across the entire spectrum, which was removed by normalization. The appearance of middle frequency depression was imposed by the normalization, owing to the increase in power from EMG in the low spatial frequency range (Figure 7, C).

An alternative investigation of the properties of the spatial  $PSD_x$  of EEG and EMG (Figures 9 and 10, frames A and C) was directed to evaluating the effects owing to the reference electrode by re-referencing (frames B and D). This was done by subtracting the spatial ensemble average of the 64 signals in each frame from each signal. The examples were from the frontal locations in subjects with eyes closed. Temporal spectral decomposition (frames A and B) was undertaken by 7 Hz band pass filtering. Spatial bands (frames C and D) were scaled logarithmically as in Figure 6, B and D.

##### Figures 9 and 10 near here #####

Compared with the subject at rest (Figure 9) the deliberate introduction of EMG increased the  $PSD_x$  power in all spatial wave lengths (Figure 10). Three components of increased EMG power were identified in all scalp locations. Component **1** was in the low spatial range ( $< .1$  cycles/cm) with temporal frequencies maximal above gamma. Component **2** was in the high spatial range ( $> .26$  cycles/cm) with temporal frequencies below theta. Component **3** was in the middle spatial range of  $.11$  to  $.4$  cycles/cm and in the beta and low gamma ranges (21 to 49 Hz).

Re-referencing acted to some extent as a high pass spatial filter with a low set point, and a high pass temporal filter with a low set point (frames B and D in Figures 9 and 10). There was a 10-fold ( $\sim 1$  log unit) reduction in relative EEG power in the low spatial frequency bands (**1**,  $< .04$  cycles/cm in  $PSD_x$ , A and B) for both EEG and EEG + EMG. There was slight smoothing in the high temporal frequencies (**1**,  $> 33$  Hz in  $PSD_t$ , C and D) for EEG + EMG (Figure 10) but not for EEG (Figure 9). There was no discernible effect on the power in the higher temporal frequencies in the mid to high spatial frequency bands (components **2** and **3**). This result indicated that some of component **1** could be attributed to EMG activity at the reference lead. Alpha was already attenuated on induction of EMG, and on re-referencing virtually disappeared from all areas, while theta activity appeared or was enhanced in the paracentral area. The results suggested that component **2** might be attenuated by a combination of a high pass temporal filter set at 4 Hz and a high pass spatial filter set at  $.1$  cycles/cm.

The effects of re-referencing and filtering on EEG and EEG + EMG were examined in the time domain. Examples from the frontal cortex are shown in Figures 11 and 12. Frame A

shows the control signals. Frame B shows the effects of re-referencing applied to diminish component **1**. Re-referencing also flattened alpha and brought deviant channels more in evidence (electrode 5). Frame C shows the effect of a high pass spatial filter set at .1 cycles/cm to mitigate component **2** of EMG. Unlike the effect of re-referencing, the reduction in activity having high temporal frequencies was often dramatic, also for EEG with little or no apparent EMG. Frame D shows the effects of high pass temporal filtering above 4 Hz to attenuate component **2** EMG. This filter removed the delta activity from the EEG but had no other discernible effect on the EEG + EMG.

##### Figures 11 and 12 near here #####

## Discussion

### 1. Network vs. holist approaches to cortex

Two analyses of cortical function may be contrasted in simplified forms. In the network approach cortex is treated as a mosaic of areas that communicate in pairwise fashion. The principal tools are time-lagged correlation, coherence and autoregression. The signals are commonly measured with linear basis functions, which give amplitude and phase relations of activity at specific frequencies. In the temporal domain the FFT is used to emphasize spectral peaks. In the spatial domain the electrodes in an array are widely spaced to collect samples from as many individual areas of the network as possible. Spatial spectra are not appropriate. In the ideal there is one frequency as the carrier signal for each message. In the holist approach cortex is viewed as a self-organizing system with space-time activity patterns that vary widely in scales of measurement. Local areas are acknowledged in terms of their privileged sensory input and motor output connections and the behavioral correlates of their activities, but not by their specific intercortical connections. Analytic basis functions are not appropriate, because the activity patterns are aperiodic, highly variable, and intrinsically unpredictable. Decomposition instead is by calculating statistical moments, nonparametric measures, PCA and ICA. Electrodes are placed in high density arrays in order to measure spatial patterns in contiguous areas. The ideal form of temporal and spatial spectra is  $1/f^2$  without significant peaks.

In practice neither approach gives results that are consistent with the ideal forms. On the one hand, while the classical frequency ranges of the EEG (Figure 3) often have impressive peaks of power, rarely do they have the form of sharp spikes indicating a single frequency. Oscillations are typically brief in duration, leading to indeterminacy of exact frequency, and bursts of oscillation show drift and modulation of the center frequency. A simple t-test

applied to evaluate the significance of group differences between spectra does so one frequency at a time in accord with the decomposition afforded by the FFT. As shown by comparing Figure 8 with Figures 9 to 11, it can give misleading results. Owing to the variance across subjects, locations and conditions, as revealed in the CV of the peak frequencies, the only differences confirmed tend to be those that were already obvious on visual inspection. The distributions of power within and between bands evidently interact and form complex relations that challenge the ingenuity of multivariate statisticians, particularly when spatial distributions become as important and informative as temporal distributions.

On the other hand, the  $PSD_t$  of both intracranial and scalp EEG occasionally give forms that are very close to the scaling ideal, especially in frontal cortex of subjects at rest, when the frontal lobes are presumably not strongly active in behavioral genesis. More often, the narrow band  $PSD_t$  excesses that comprise peaks in the classical ranges obscure the  $1/f^\alpha$  form to the extent that measurements of the slope,  $\alpha$ , are not reliable. The  $PSD_x$  of epipial EEG conforms to the  $1/f^\alpha$  ideal (Freeman et al., 2000), but  $PSD_x$  from scalp EEG do not (Figure 13). This distortion is likely to be due to the smoothing effects of the intervening dura, skull and soft tissues in the volume conductor on the middle and high spatial frequencies. It does not constitute evidence against scaling. It appears that some peaks consistent with the size of gyri persist despite the severe smoothing in the middle range. This finding justifies continuing intensive search in that range. Spatial oversampling provides a basis for low pass spatial filtering to attenuate noise, which comes from individual electrodes, and which is evident in the high spatial spectral range.

##### Figure 13 near here #####

The network and holist approaches found common ground in the two spatiotemporal spectral patterns that were identified by decomposition into spectral bands. Peaks in  $PSD_t$  associated with low spatial frequencies in  $PSD_x$  manifested widespread synchrony in the alpha, beta and gamma ranges, as reported in numerous studies on scalp EEG. The frequencies within the peaks were time-varying, and the covariances extended well beyond pairs of discrete areas, but the concept of information shared by narrow-band transmission could hold for both holist and network models. Peaks in the middle spatial frequency range of  $PSD_x$  in association with broadly distributed temporal frequencies in  $PSD_t$  manifested temporal spikes (impulses) occurring synchronously across wide regions of cortex. Evidence has been derived from EEG studies in animals that spatially coherent temporal spikes may manifest time markers for synchronizing pulses that trigger repeated and widespread phase transitions in cortex (Freeman and Rogers, 2001, in press). This staccato mode of holist operation was suggested also by the shifting dipole found in scalp EEG by Lehmann and Michel (1990). The dipole displayed sudden jumps at intervals in the theta range. Irrespective of whether cortex operates as a network of modules or as a self-organizing tissue providing for global integration, some neural clock mechanism for large-scale synchronization in ultra-short time periods appears to be necessary. High density arrays for recording scalp EEG offer an important and perhaps crucial source of information to guide the search for such a mechanism.

## 2. Behavioral correlation

The search for spatial structure in the EEG was conducted in the spatial frequency domain by focusing on concentrations of  $PSD_x$  power in selected spatial frequency bands. The greatest power was in the low frequency band ( $<.1$  cycles/cm) in all subjects, sites and conditions, often but not always in proportion to the  $1/f^2$  power-law scaling with temporal frequency. Of particular interest was the appearance in 6 of 9 subjects in the eyes closed

condition of peaks of  $PSD_x$  power in the mid-range (.1 to .4 cycles/cm) in association with alpha. When on command these subjects opened their eyes in the dark, the alpha was replaced by theta activity, and local peaks were seen more clearly in the middle range of "texture". Theta appeared *de novo* in two other subjects with little prior alpha. When present these small peaks extended across all temporal bands from delta to gamma at the same spatial frequency and often at the same level of power independently of temporal frequency. The peaks were seen most clearly in  $PSD_x$  of the paracentral EEG and less so in the occipital area. Alpha power was not usually seen in the frontal area, and when it was, it was not associated with mid-range spatial spectral peaks. The temporal peak of frontal alpha but not that of paracentral or occipital alpha was removed by re-referencing, suggesting that frontal alpha originated posteriorly and either spread by volume conduction or appeared at the referential lead on the vertex. The fact that alpha diminished in most sites while theta increased also with voluntary induction of EMG suggested an association with the intentional act, either holding the eyes open or sustaining a controlled level of EMG.

### 3. EEG vs. EMG

A basic tenet of signal detection theory is that an adaptive filter must be fitted to detect and identify any significant additive non-white noise (known as "clutter" by radar technicians) simultaneously with a filter fitted to the signal. The difficulty of separating signal, clutter and noise is compounded by the fact that the induction of an intentional act is accompanied by changes in the EEG, so that not all of the differences illustrated in Figures 9 to 12 are due to additive noise. Some are due to changes in brain state. After EEG differences between the states of eyes closed and open were characterized, the approach used here was to distinguish three spectral ranges as components of the EMG.

Component 1 most clearly departed from the  $1/f^2$  form in the gamma range of the  $PSD_t$ . It was somewhat reduced by re-referencing (frame D in Figure 9, and frame B in Figure 12), so it could be attributed in part to activity from the referential lead. Component 1 also had substantial power in the low range of the  $PSD_x$ , which might be explained by summing and smoothing of muscle action potentials in the scalp volume conductor. High pass spatial filtering (cutting off below .1 cycles/cm) reduced the low spatial frequency power and also the activity in the high temporal frequency range (frame C in Figure 12). However, the dramatic reduction in activity with high temporal frequencies indicated that such a high pass spatial filter also unfortunately reduced the in-phase component of gamma activity. That "zero time lag" gamma component has been the object of intensive investigation for many investigators working with human gamma activity, in order to establish widespread spatial coherence of cortical activity in the gamma band in relation to human cognition (Müller, et al., 1996; Tallon-Baudry et al. 1998; Miltner et al. 1999; Rodriguez et al. 1999; Müller 2000). In animal cognition the common wave form of gamma activity in sensory cortices was shown to serve as a carrier wave for cognitive information (Barrie, Freeman and Lenhart, 1996; Freeman, 2000), which was expressed by amplitude modulation of the carrier. The application of high pass spatial filter would remove the carrier wave, but it might retain and perhaps enhance the modulations, so that the high pass spatial filter deserves further study using behavioral correlates.

Component 2 contained substantial EMG power at high spatial frequencies and low temporal frequencies. This phenomenon might also be explained by the summation of propagated muscle potentials in the scalp volume conductor, which could give rise to sustained low frequency power owing to smoothing by temporal dispersion (as with compound action potentials), while retaining some fine spatial texture, owing to the proximity of muscle fibers to the array electrodes. Accordingly, a high pass temporal filter set at a low temporal frequency (cutting off below 4 Hz) was tested to see whether it

reduced this EMG contribution, thereby improving access to the high frequency spatial texture of the gamma activity recorded at the scalp (Figure 12, frame D). Little or no improvement was noted.

Component **3** occupied the middle spatial range of the  $PSD_x$  and included both beta and gamma activity in the  $PSD_t$ . Owing to this overlap and commingling, doubts have often been expressed that scalp recordings can give any useful information about human gamma oscillations in relation with behavior. Sheer (1976) introduced a method for detecting gamma by narrow band pass filtering at 35-45 Hz, on the premise that gamma oscillations were focused at 40 Hz. As a control he and others (e.g., Haig et al., 2000). also measured the power in an adjacent pass band (e.g. 45-55 Hz) to estimate EMG power. In the absence of concentration of power at 40 Hz in the majority of subjects under the condition of rest, there was no basis for using Sheer's method in the present study to separate EEG from EMG. When narrow band 40 Hz did occur, that method had the disadvantage of introducing ringing of narrow band pass filters in response to random spike activity covering the spectral vicinity. It also reduced temporal resolution by the persistent ringing. In prior animal studies the narrow band oscillations at or near 40 Hz, when present prior to action, tended to disappear when the animals become active in a behavioral task (Sanes and Donoghue, 1993; Gram et al., 2001; Murthy and Fetz, 1996; Kay and Freeman, 1998). The results presented here did not support the use of narrow band temporal filtering. The conclusion is that the best recourse in regard to EMG is prevention. The log-log display of  $PSD_t$  can provide an assay for EMG by means of which to train subjects and clinicians in detecting and minimizing it by systematic relaxation and muscle control.

#### **4. Spatial sampling**

If the mid-range spatial spectral peaks were to be targets for further exploration, then the upper limit of their frequency range, .4 cycles/cm (2.5 cm/cycle), would be taken as the highest spatial frequency expected to exceed the noise level. According to the rule that the sample frequency should be 3 to 5 times higher than that limit (Barlow, 1993), the electrode spacing would be 5 to 8 mm, which would be 2 to 3 times wider than the 3 mm interval used in this study and about 1/3 of the 3 cm interval cm previously suggested (Spitzer et al., 1980; Srinivasan, Tucker and Murias, 1998).

This small interval (high spatial sample rate) may at first sight seem to be inappropriate for scalp recording, owing to theoretical and experimental derivations of a wider optimal sample interval (Nunez, 1981; Nunez et al., 1997; Srinivasan, Nunez and Silberstein, 1998; Burkitt et al., 2000). Wingeier et al. (2001) and Nunez et al. (1997) have shown that cortical EEG generators as shallow as 15 mm from the scalp may give detectable components at electrodes up to 10 cm or more distant. The brain coverings smooth the EEG texture observed subdurally from electrodes on the pia (Figure 13), and distort the  $1/f^{\alpha}$  relation seen at the pia (Freeman et al., 2000). Indeed, restoration of the  $1/f^{\alpha}$  form of the spatial spectrum might provide a useful criterion for evaluating transforms used to compensate for the effects of volume conduction, if the slope,  $\alpha$ , can be measured reliably. However, analysis of spatial patterns of cortical EEG recorded intracranially in animals (Freeman, 2000) has shown that, despite electrode spacing (0.5-0.8 mm) that is less than the point spread function (0.6-1.0 mm) of cortical generators (Freeman, 2000) and still substantially larger than the size of cortical columns (0.125 mm) and hypercolumns (1.0 mm), each electrode can and does contribute to the classification of AM patterns of EEG (Barrie, Freeman and Lenhart, 1996; Ohl, Scheich and Freeman, 2001). This efficacy is due to the fact that the information subserving measurement and classification is spatially distributed, and each electrode contributes independently and equally to the task, irrespective of its location as long as it is located within the coherent domain of recording.

In conclusion, on the one hand, if the aim of spatial analysis is to use scalp EEG to localize spatial sources of cortical signals, such as epileptic foci or components of event related potentials, then little is gained in resolution by close spacing, and much is lost by confining the available number of electrodes to a small area. On the other hand, if the aim of recording is to extract the nonlocal information in the EEG that is cognitively related, then high spatial sampling rates are desirable. Furthermore, if in accordance with the theory of self-organized criticality (Bak et al., 1987; ingber, 1995; Hwa and Ferree, 2002) EEG phenomena are fractal, estimates of the size of coherent domains may vary with the sizes spatial intervals used for observation, which further enjoins the need for high density arrays.

## References

- Bak P, Tang C, Wiesenfeld K. Self-organized criticality: an explanation of  $1/f$  noise. *Physical Rev. Lett.* 1987, 59: 364-374.
- Barlow JS. *The Electroencephalogram: Its Patterns and Origins.* Cambridge MA: MIT Press, 1993.
- Barrie JM, Freeman WJ, Lenhart M. Modulation by discriminative training of spatial patterns of gamma EEG amplitude and phase in neocortex of rabbits. *J. Neurophysiol.* 1996, 76: 520-539.
- Bressler SL. Interareal synchronization in the visual cortex. *Behav. Brain Res.* 1996, 76: 37-49
- Bressler SL, Coppola R, Nakamura R. Episodic multiregional cortical coherence at multiple frequencies during visual task performance. *Nature* 1993, 366: 153-156.
- Burkitt GR, Silberstein RB, Cadusch PJ, Wood AW. Steady-state visual evoked potentials and traveling waves. *Clin. Neurophysiol.* 2000, 111: 246-258.
- Calvin WH. *The Cerebral Code. Thinking a Thought in the Mosaics of the Mind.* Cambridge MA: MIT Press, 1996.
- Dumenko VN. The functional significance of high-frequency components of brain electrical activity. In: *Complex Brain Functions: Conceptual Advances in Russian Neuroscience.* Miller R, Ivanitzky I, Balaban P (eds.). Amsterdam NL: Harwood Acad. Publ., 2000, pp. 129-150.
- Freeman WJ. Use of spatial deconvolution to compensate for distortion of EEG by volume conduction. *IEEE Trans. Biomed. Engin.* 1980, 27: 421-429.
- Freeman WJ. *Neurodynamics. An Exploration of Mesoscopic Brain Dynamics.* London UK: Springer-Verlag, 2000.
- Freeman WJ. *Neurodynamics. An Exploration of Mesoscopic Brain Dynamics.* London UK: Springer-Verlag, 2000.

- Freeman WJ, Baird B. Relation of olfactory EEG to behavior: Spatial analysis: *Behav. Neurosci.* 1987, 101: 393-408.
- Freeman WJ, Barrie JM Analysis of spatial patterns of phase in neocortical gamma EEGs in rabbit. *J. Neurophysiol.* 2000, 84: 1266-1278.
- Freeman WJ, Rogers LJ. Fine temporal resolution of analytic phase reveals episodic synchronization by state transitions in gamma EEGs. *J. Neurophysiol.* 2001, 87: 937-945.
- Freeman WJ, Rogers LJ. Episodic synchronization of gamma activity across multiple cortices revealed by the Hilbert transform. *Intern. J. Bifurcation Chaos*, 2003, in press.
- Freeman WJ, Rogers LJ, Holmes MD, Silbergeld DL. Spatial spectral analysis of human electrocorticograms including the alpha and gamma bands. *J. Neurosci. Meth.* 2000, 95: 111-121.
- Gevins A, Smith ME, McEvoy L, Yu D. High resolution EEG mapping of cortical activation related to working memory: effects of task difficulty, type of processing, and practice. *Cerebral Cortex* 1997, 7: 374-385.
- Gonzalez RC, Wintz P. *Digital Image Processing*. Reading MA: Addison-Wesley, 1977.
- Haig AR, Gordon E, Wright JJ, Meares RA, Bahramali H. Synchronous cortical gamma-band activity in task-relevant cognition. *NeuroReport* 2000; 11: 669-675.
- Hall EL. *Computer Image Processing and Recognition*. New York: Academic Press, 1979. Sampling theorem: pp. 89-94. Shannon theory: pp. 312-317.
- Hwa RC, Ferree T. Scaling properties of fluctuations in the human electroencephalogram. *Physical Rev.* 2002, E 66: 021901.
- Ingber L. Statistical mechanics of multiple scales of neocortical interactions. In: Nunez PL, *Neocortical Dynamics and Human EEG Rhythms*. New York NY: Oxford University Press 1995, pp. 628-681.
- Kay LM, Freeman WJ. Bidirectional processing in the olfactory-limbic axis during olfactory behavior. *Behav. Neurosci.* 1998, 112: 541-553.

- Lachaux JP, Rodriguez E, Martinerie J, Varela FJ. Measuring phase synchrony in brain signals. *Human Brain Mapping*, 1999, 9:194-208.
- Lehmann D, Michel CM. Intracerebral dipole source localization for FFT power maps. *Electroenceph. clin. Neurophysiol.* 1990, 76: 271-276.
- Linkenkaer-Hansen K, Nikouline VM, Palva JM, Ilmoniemi RJ. Long-range temporal correlations and scaling behavior in human brain oscillations. *J. Neurosci.* 2001; 15: 1370-1377.
- Mingzhou D, Bressler SL, Yang W, Liang H. Short-window spectral analysis of cortical event-related potentials by adaptive multivariate autoregressive modeling: data preprocessing, model validation, and variability assessment. *Biol. Cybern.* 2000, 83: 35-45.
- Miltner WHR, Barun C, Arnold M, Witte H, Taub E. Coherence of gamma-band EEG activity as a basis for associative learning. *Nature* 1999, 397: 434-436.
- Müller MM, Bosch J, Elbert T, Kreiter A, Valdes Sosa M, Valdes Sosa P, Rockstroh B. Visually induced gamma band responses in human EEG - A link to animal studies. *Exper. Brain Res.* 1996, 112: 96-112.
- Müller MM. Hochfrequente oszillatorische Aktivitäten im menschlichen Gehirn. *Zeitschrift für Exper. Psychol.*, 2000 47: 231-252.
- Murthy VN, Fetz EE. Oscillatory activity in sensorimotor cortex of awake monkeys: Synchronization of local field potentials and relation to behavior. *J. Neurophysiol.* 1996, 76: 3949-3967.
- Nunez PL. *Electric Fields of the Brain: The Neurophysics of EEG*. New York: Oxford Univ. Press, 1981.
- Nunez PL, Srinivasan R, Westdorp AF, Wijesinghe RS, Tucker DM, Silberstein RB, Cadusch PJ. EEG coherency I: statistics, reference electrode, volume conduction, Laplacians, cortical imaging and interpretation at multiple scales. *Electroenceph. clin. Neurophysiol.* 1997, 103: 499-515.

- Ohl FW, Scheich H, Freeman WJ. Change in pattern of ongoing cortical activity with auditory category learning. *Nature* 2001, 412: 733-736.
- Oram MW, Hatsopoulos NG, Richmond BJ, Donoghue JP. Excess synchrony in motor cortical neurons provides redundant direction information with that from coarse temporal measures. *J. Neurophysiol.* 1996, 86: 1700-1716.
- Quiroga RQ, Krasov A, Kreuz T, Grassberger P. Performance of different synchronization measures in real data: A case study on electroencephalographic signals. *Physical Rev. E* 2002 65: 041903.
- Quiroga RQ, Schürmann M. Functions and sources of event-related EEG alpha oscillations studied with the Wavelet Transform. *Clin. Neurophysiol.* 1999, 110: 643-654.
- Rodriguez E, George N, Lachaux J-P, Martinerie J, Renault B, Varela F. Perception's shadow: long-distance synchronization of human brain activity. *Nature* 1999, 397: 430-433.
- Sanes JN, Donoghue JP. Oscillations in local field potentials of the primate motor cortex during voluntary movement. *Proc. Nat'l. Acad. Sci. USA* 1993, 90: 4470-4474.
- Sheer D. Focused arousal in 40-Hz EEG. In: Knight RM, Bakker DJ. (eds.) *The Neuropsychology of Learning Disorders*. Baltimore: Univ. Park Press, 1976, pp. 71-87.
- Singer W, Gray CM (1995) Visual feature integration and the temporal correlation hypothesis. *Ann. Rev. Neurosci.* 1995, 18: 555-586.
- Spitzer AR, Cohen LG, Fabrikant J, Hallett M. A method for determining optimal interelectrode spacing for cerebral topographic mapping. *Electroenceph. clin. Neurophysiol.* 1980; 72: 355-361.
- Srinivasan R, Nunez PL, Silberstein RB. Spatial filtering and neocortical dynamics: estimates of EEG coherence. *IEEE Trans. Biomed. Engin.* 1998, 45: 814-826.
- Srinivasan R, Tucker DM, Murias M. Estimating the spatial Nyquist of the human EEG. *Behavioral Research Methods, Instruments and Computers* 1998; 30: 8-19.

- Tallon-Baudry C, Bertrand O, Delpuech C, Pernier J. Stimulus-specificity of phase-locked and non phase-locked 40-Hz visual responses in human. *J. Neurosci.* 1996, 16: 4240-4249.
- Tallon-Baudry C, Bertrand O, Peronnet F, Pernier J. Induced gamma-band activity during the delay of a visual short-term memory task in humans. *J. Neurosci.* 1998, 18: 4244-4254.
- Taylor JG. Neural networks for consciousness. *Neural Networks* 1997, 10: 1207-1225.
- Wingeier BM, Nunez PL, Silberstein RB. Spherical harmonic decomposition applied to spatial-temporal analysis of human high-density electroencephalogram. *Physical Rev. E* 2001; 64: 051916.
- Varela F, Lachaux J-P, Rodriguez E, Marinerie J. The brainweb: Phase synchronization and large-scale integration. *Nature Rev. Neurosci.* 2: 229-239.

## Figures

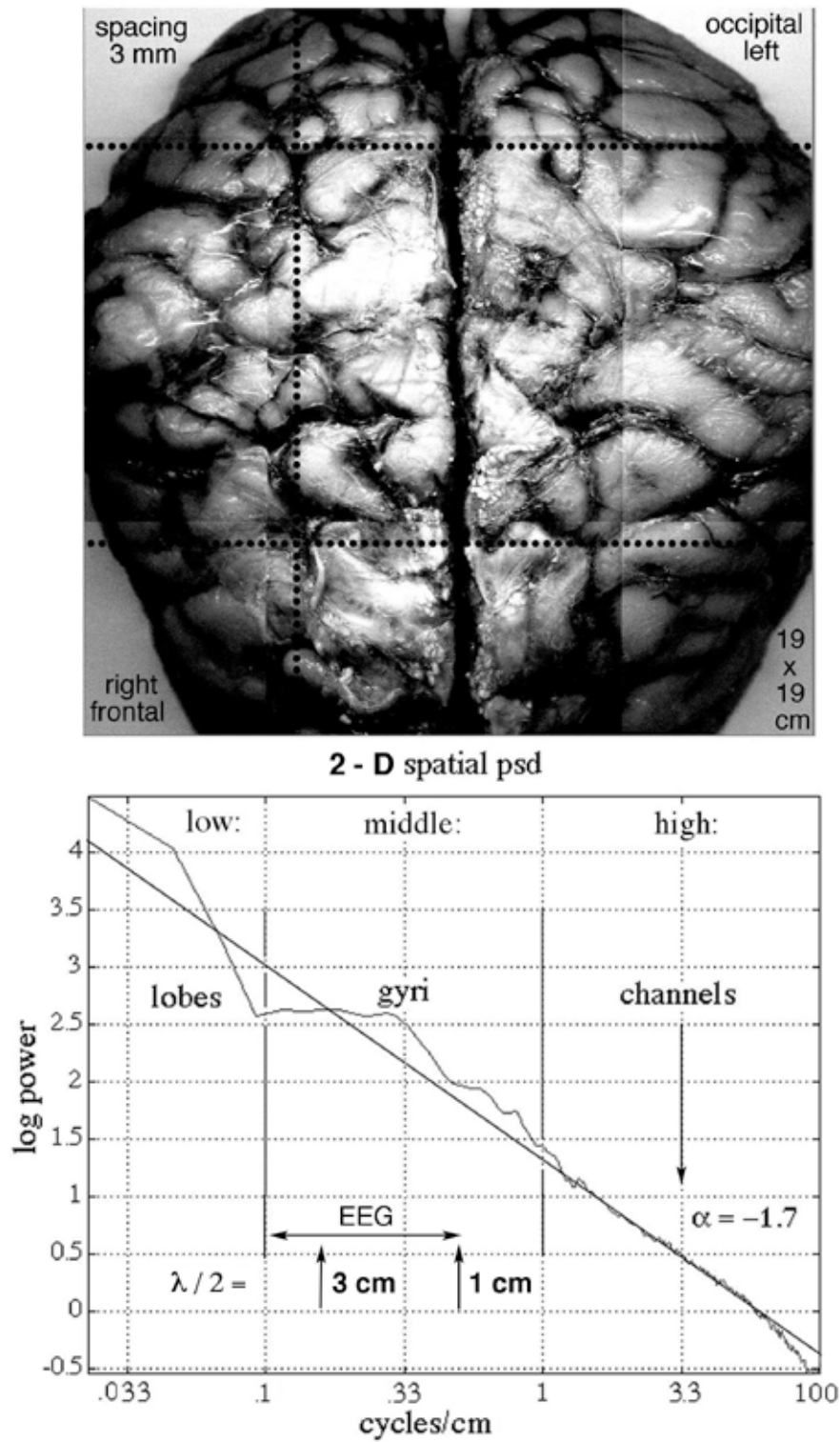


**Figure 1. Upper frame:** A montage of photographs shows the surface of a human brain specimen from a teaching collection. The light areas are gyri, and the dark lines are sulci. The scale has been expanded from the radius of the brain, 7.5 cm, to the radius of the

scalp, 9.0 cm. The rows of dots show three locations of the 64x1 array of scalp electrodes. **Lower Frame:** The 2-dimensional Fourier transform was taken at 1 mm digitizing steps of the photograph for the spatial power spectral density,  $PSD_x$ . The central peak corresponds to the typical length (3 cm) and width (1 cm) of gyri, and to a peak in the  $PSD_x$  of the EEGs.

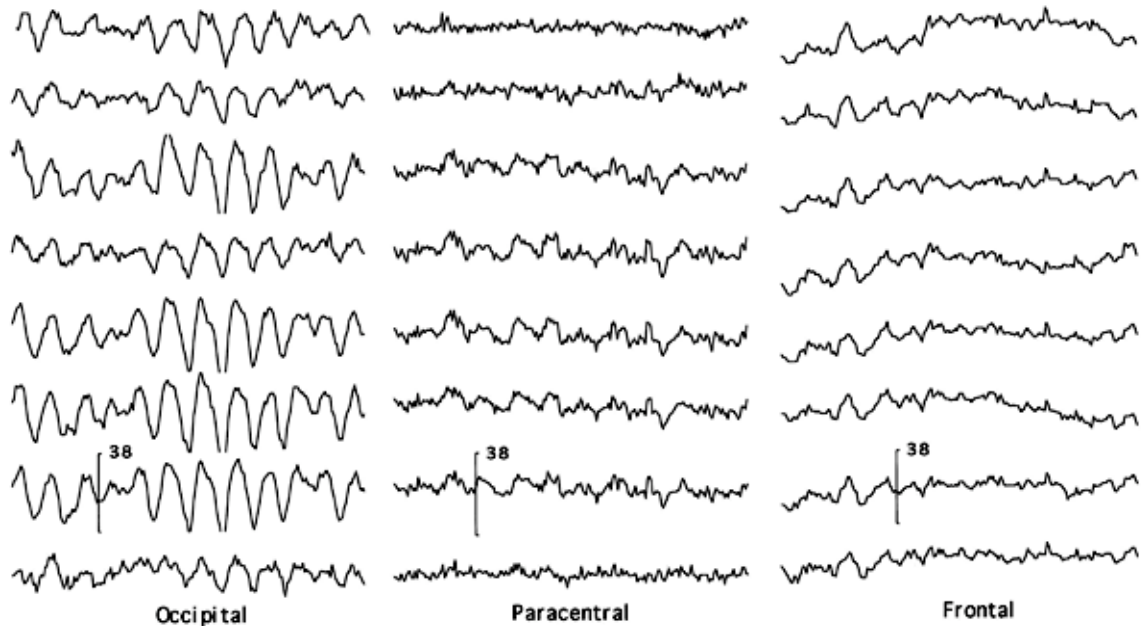


**Figure 2.** Representative EEG recordings are shown from 8 consecutive electrodes in a subject at rest with eyes closed. The 18.9 cm array was placed successively over the midline occipital and frontal areas and across the central sulcus over the right frontoparietal area, 1 to 64 front to back. Interval: 3 mm. Duration: 1 s. Amplitude: microvolts.

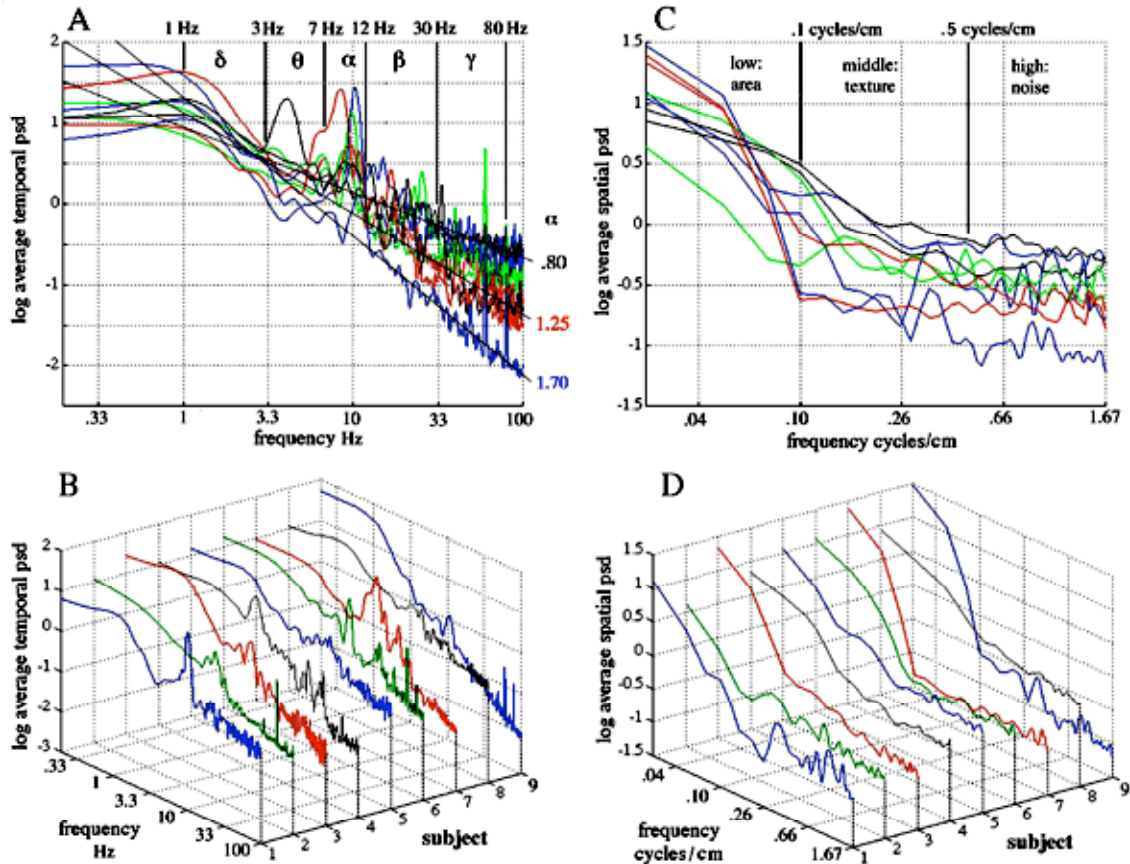


**Figure 3. A, B.** The  $1/f^{\alpha}$  form was displayed in coordinates of log power and log frequency. Deviations from that ideal occurred as peaks in the classical ranges (as defined in this report). The lowest spectrum (blue) shows a typical '40 Hz' peak as well as 60 Hz and 80 Hz artifacts. The concave-upward curvature of some other spectra in the gamma range shows power in excess of  $1/f^{\alpha}$  suggesting occult EMG.

$\alpha$ : frontal  $1.78 \pm 0.76$ ; occipital  $1.19 \pm 0.28$

**C, D.** The spatial spectra do not conform to  $1/f^{\alpha}$ . Reasons are given in this report to propose that the middle range reveals significant textures in spatial patterns of scalp EEG at scales corresponding to the length ( $\sim 3$ -5 cm) and width ( $\sim 1$  cm) of human gyri (Freeman et al., 2000).

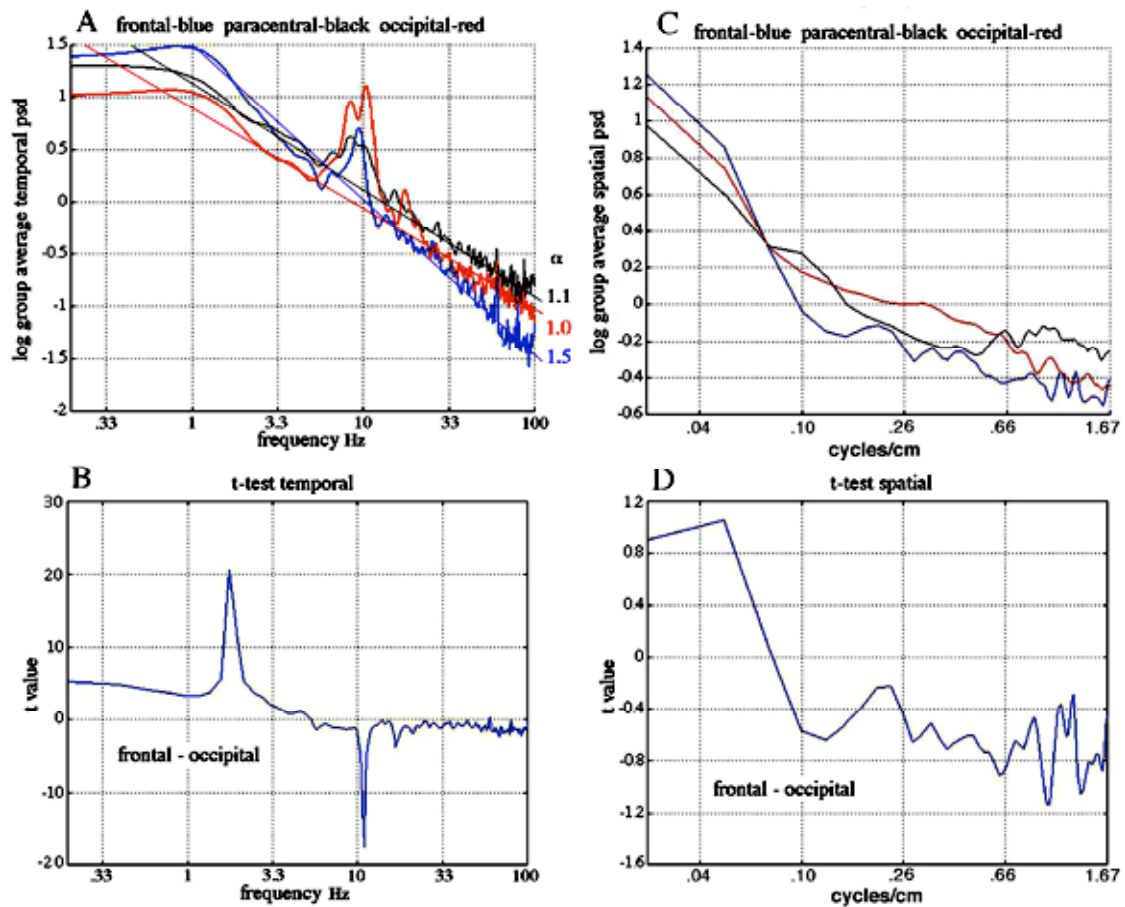


**Figure 4.** **A.**  $PSD_t$  from 4 subjects were average before taking the logarithm for comparison across locations. **B.** The group mean t-test revealed dominance of frontal delta and occipital alpha. **C, D.**  $PSD_x$  did not vary significantly by location.

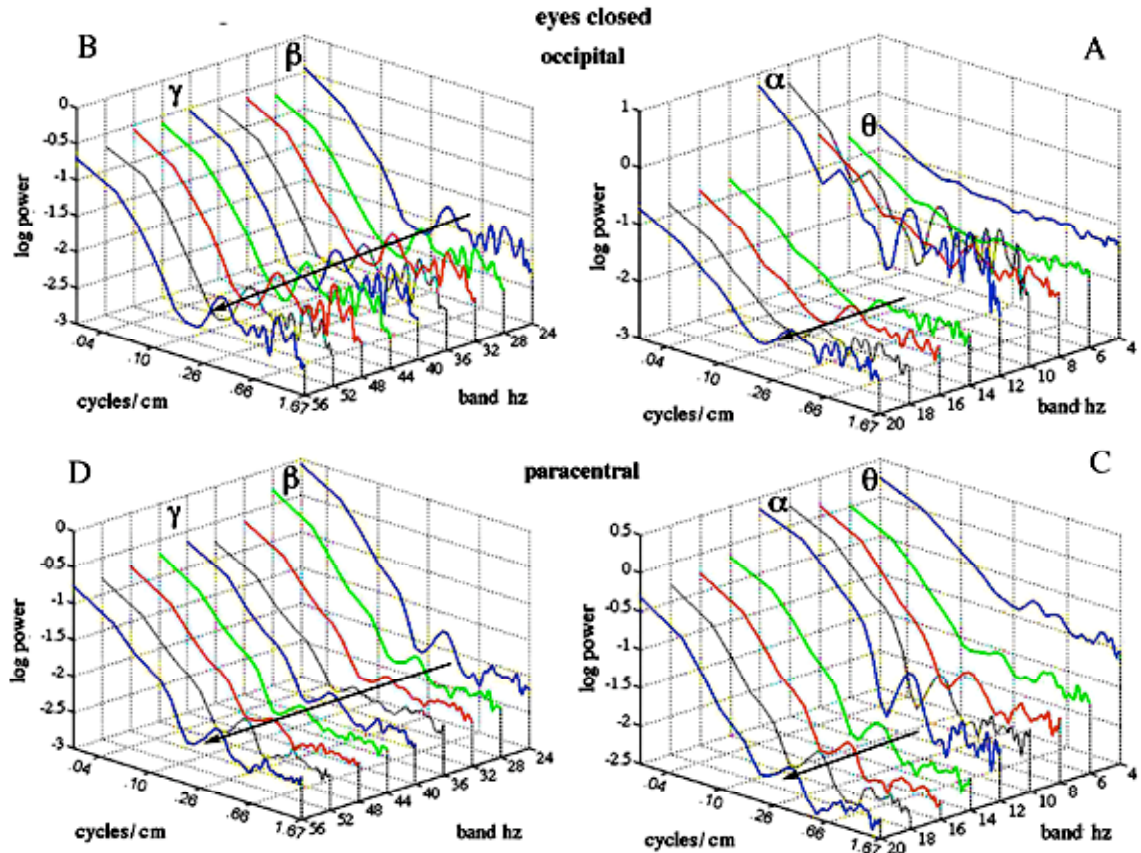


**Figure 5.** The fine structure of spectra was revealed by decomposition into bands. The bands were displayed with frequency increasing right to left, because the power usually diminishes with frequency. The two ranges were separated to accommodate the change in scale. Examples are shown of 2 recurring patterns. (1) A high alpha or theta peak at low spatial frequency (**A**, **C**) indicated broad spatial synchrony. (2) A high peak of alpha (**A**) or theta (**C**) in the  $PSD_t$  was usually accompanied by a middle-range peak in the  $PSD_x$  that extended across the  $PSD_t$  (**B**, **D**) with nearly constant amplitude and spatial frequency. This pattern of deviation from  $1/f^2$  indicated that the power in synchronized alpha and theta waves had spatial texture in half-wave lengths of 1.25 to 5 cm.

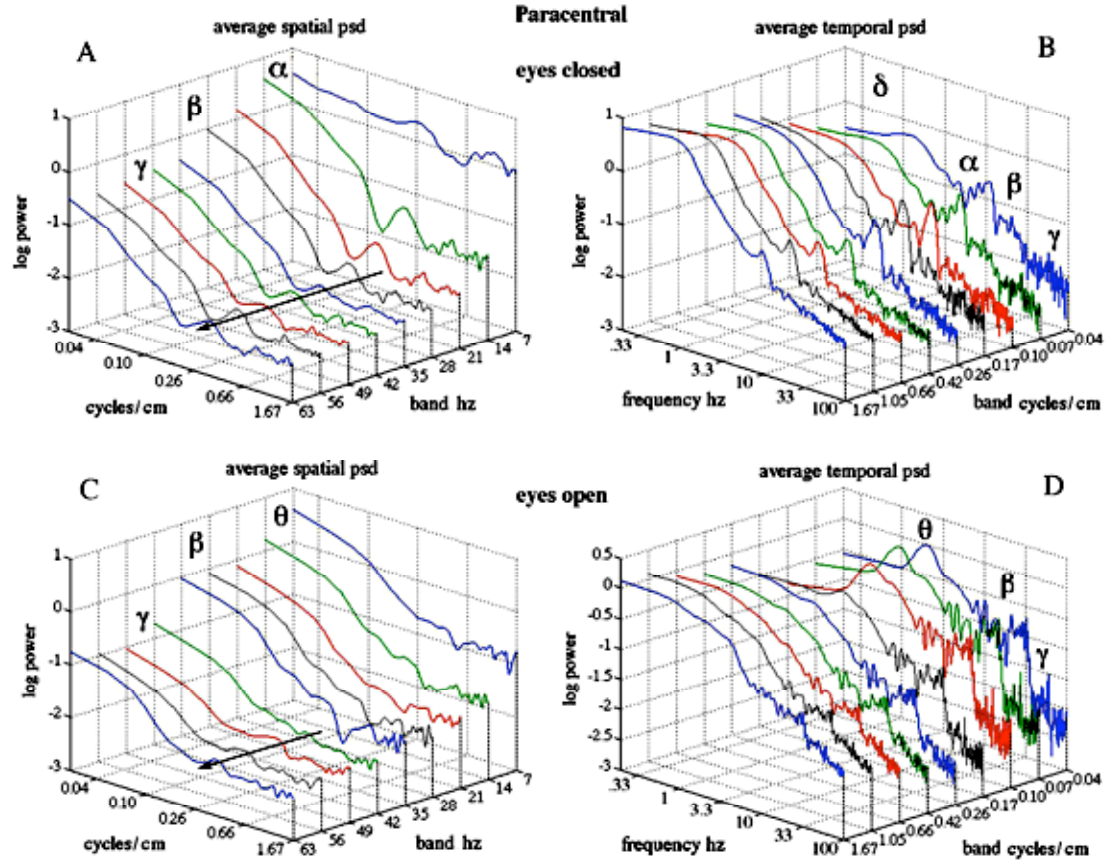


**Figure 6.** The characteristic spectral changes are illustrated from eyes closed to open. **A**, **C**.  $PSD_x$  are decomposed by temporal band. **B**, **D**.  $PSD_t$  are decomposed by spatial bands. Alpha is overtaken or replaced by theta in peaks that extend at least up to .4 cycles/cm. Beta activity increases in amplitude especially in the low and middle frequency ranges, indicating spatial synchrony and texture. The middle-range spatial peaks in the gamma range show little change.

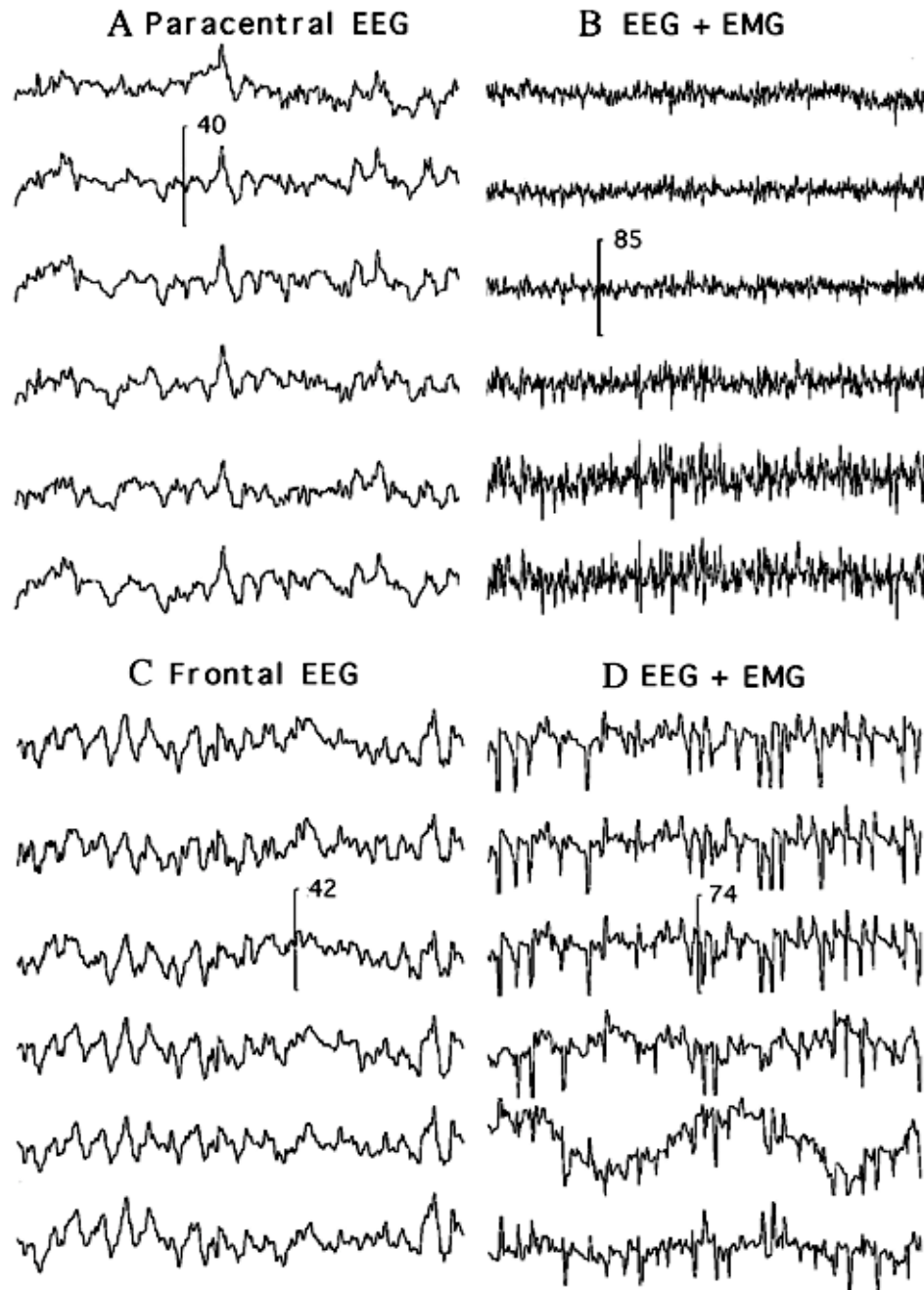


**Figure 7. Left:** Examples are shown of 6 of 64 EEG from two subjects with eyes closed, awake, relaxed, aiming to minimize EMG and movement artifacts. **Right:** The subjects maintained low-level EMG. Duration: 1 s. Amplitude: microvolts.

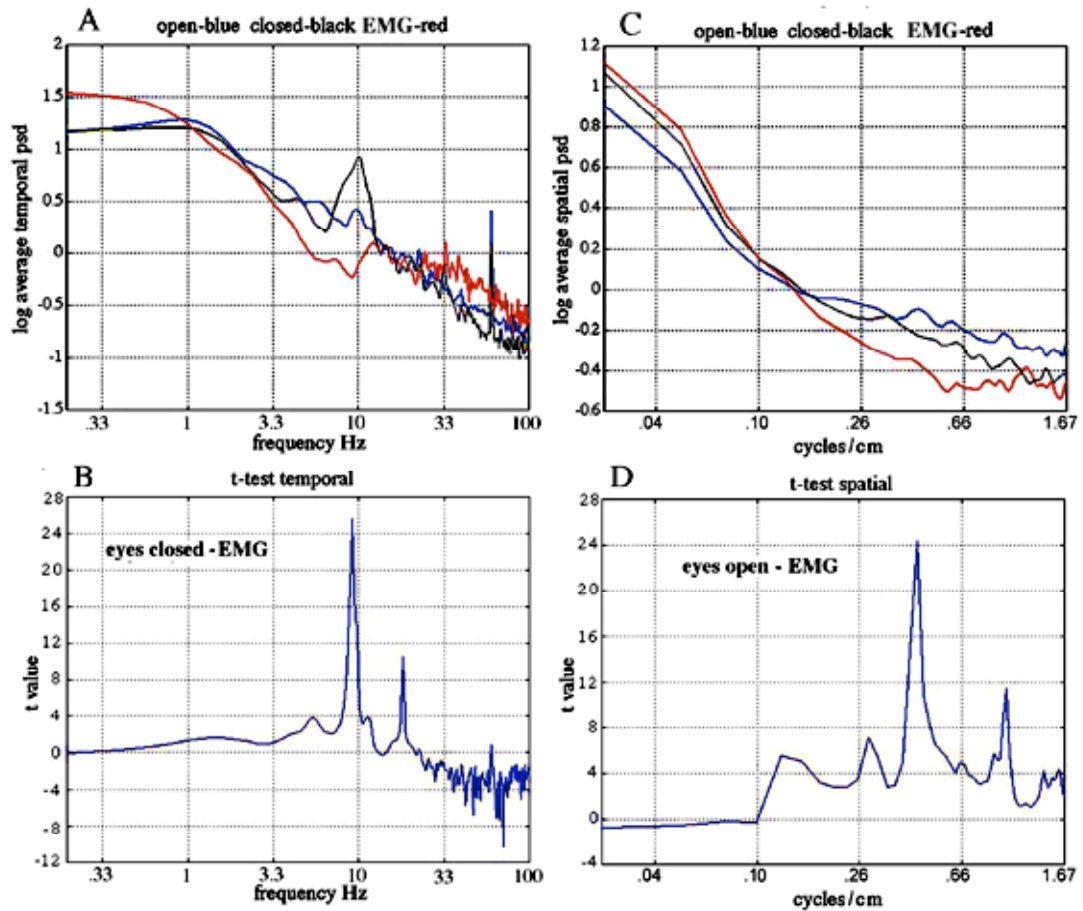


**Figure 8.** Comparison of pooled spectra point-wise at each frequency was not very informative. **A.** Averages of normalized  $PSD_t$  from 4 subjects (Figure 4) showed disappearance of alpha on opening the eyes (blue) or inducing EMG and a significant departure from the  $1/f^2$  form (red). **B.** A pooled t-test confirmed only the change for eyes closed - EMG. **C.** The  $PSD_x$  were normalized to remove subject differences and the global increase in amplitude from added EMG. This distorted the comparison, because the greatest increase with EMG was in the low spatial range, so that the middle range seemed relatively depressed. **D.** A pooled t-test high-lighted a difference at or near .4 cycles/cm only for eyes open - EMG.

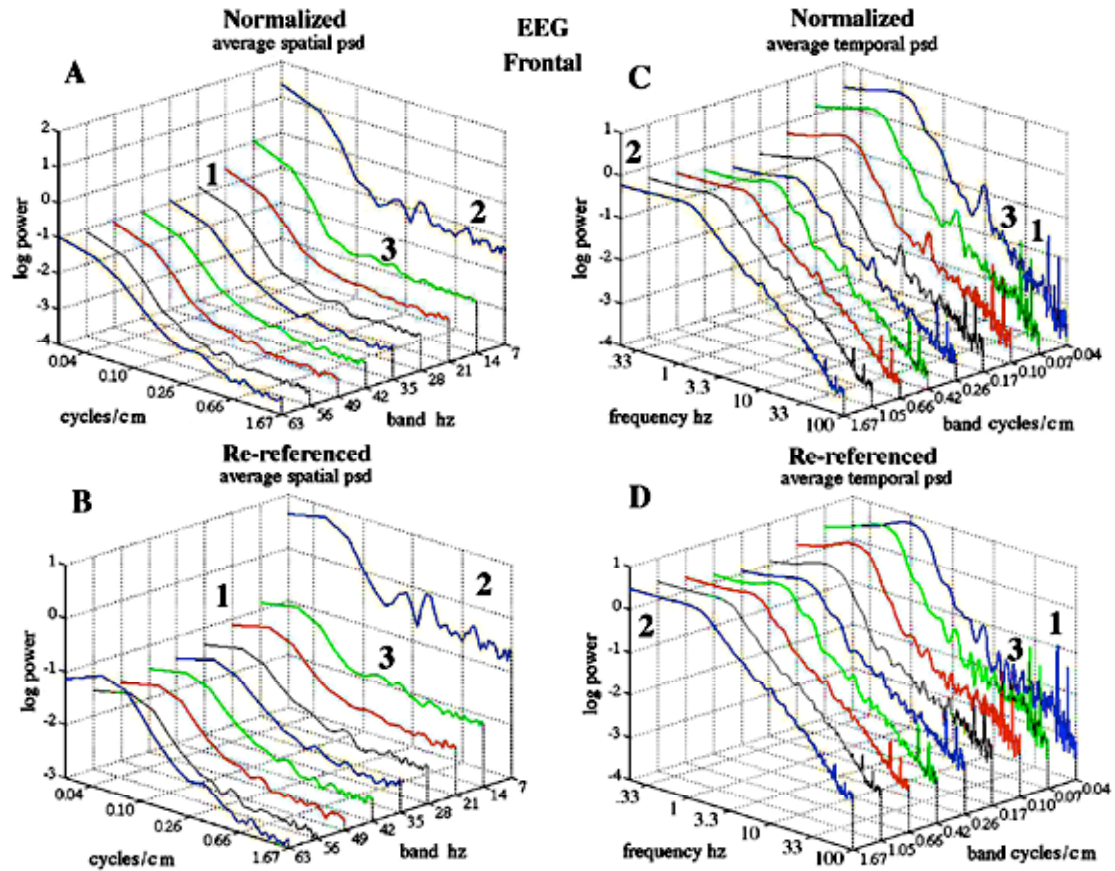


**Figure 9.** The effect on EEG of re-referencing is shown for comparison with the three components of the EMG (shown in Figure 10). **A.** The average  $PSD_x$  is decomposed in non-overlapping temporal frequency bands 7 Hz wide. **B.** The low spatial frequencies are selectively attenuated by re-referencing except at 60 Hz, which varied by channel. **C.** The  $PSD_t$  of EEG showed a good approximation to the  $1/f^2$  form under decomposition by spatial spectral bands. **D.** Re-referencing attenuated frontal alpha and the low spatial frequencies. Under normalization the high spatial frequencies appeared to be enhanced.

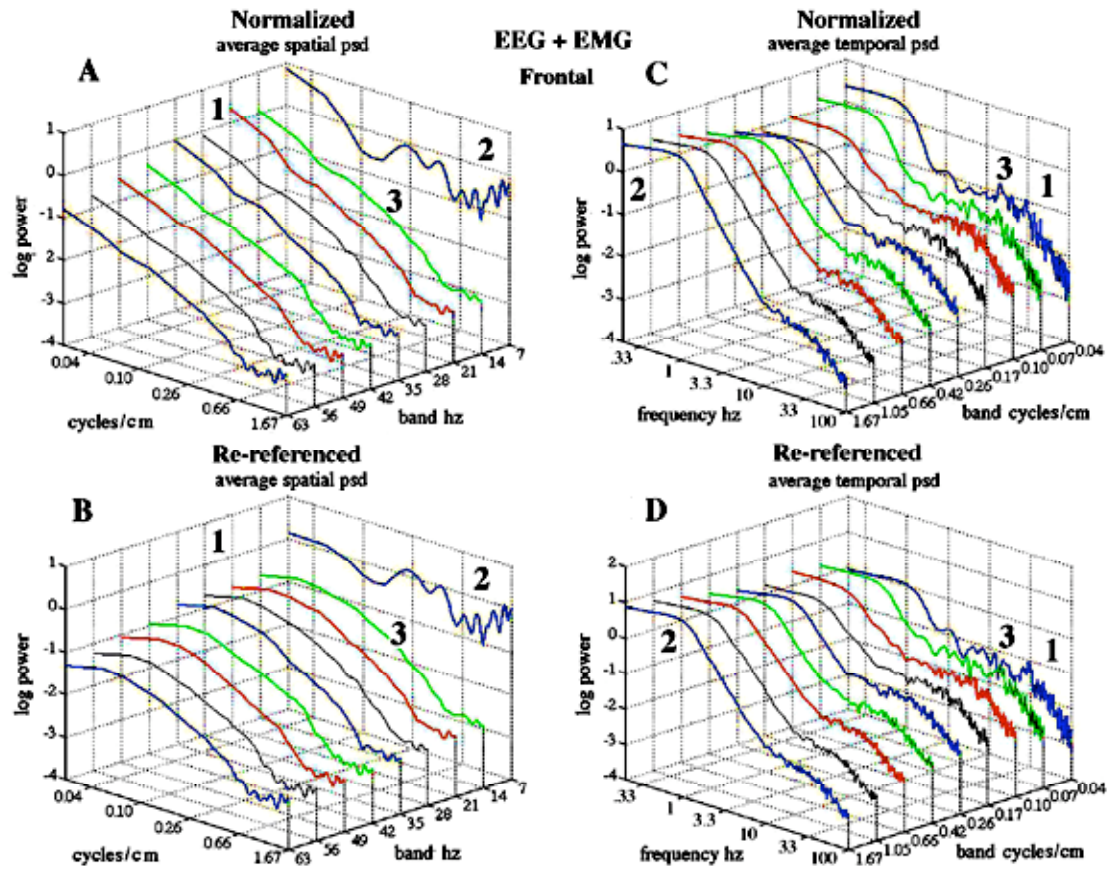


**Figure 10.** The spectral changes with addition of EMG are illustrated. **A.** The relative power in the middle range of the  $PSD_x$  was increased (**3**), but the form was not  $1/f^2$ . **B.** Re-referencing decreased power in the low frequency range (**1**). **C.** EMG increased power in the gamma range (**1**) not with the  $1/f^2$  form. **D.** Re-referencing decreased power in the low spatial range, not the high range (**2**), and mitigated the added EMG power in the high temporal range (**1**). The departure from the  $1/f^2$  form in the gamma range (**1**) could provide a useful measure of EMG for biofeedback training of subjects to decrease occult EMG.

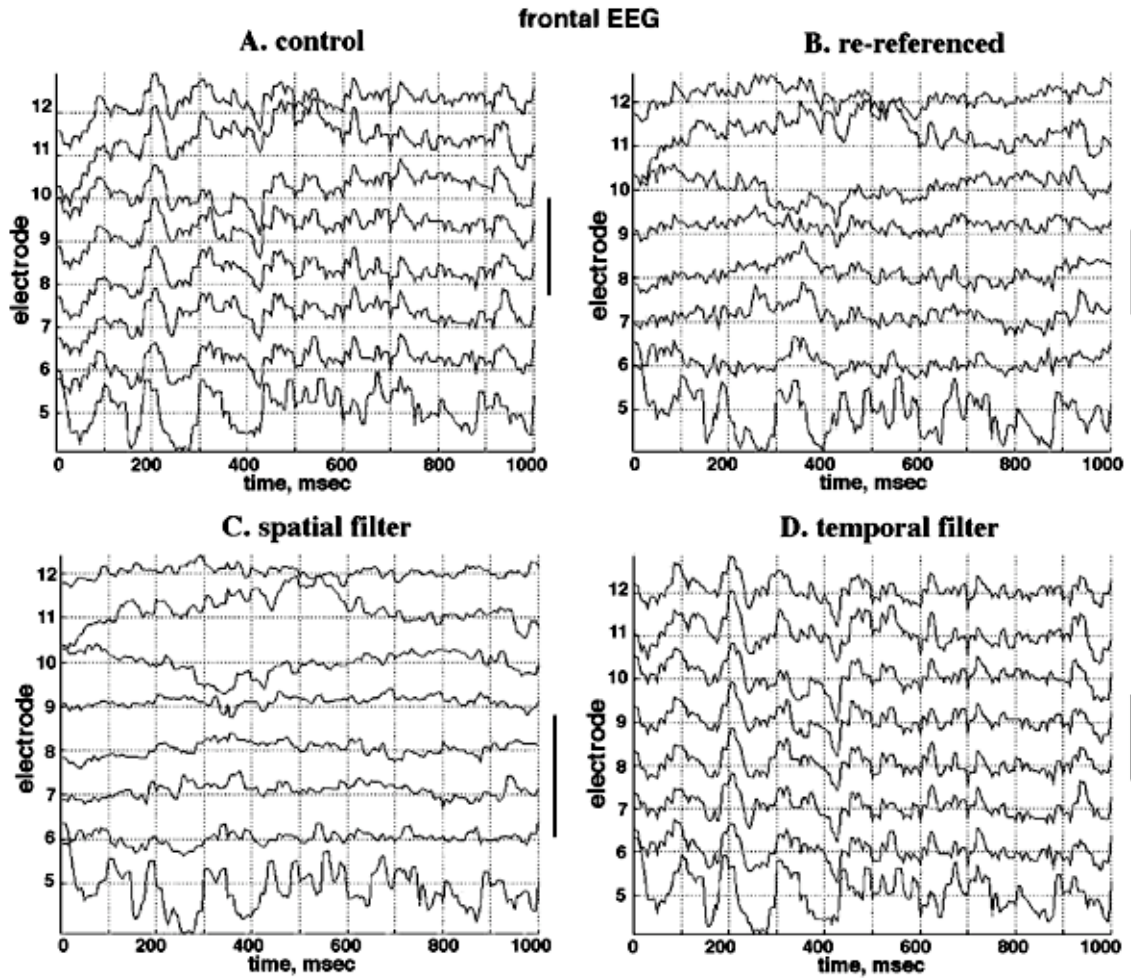


**Figure 11.** The effects on EEG (frontal, eyes closed) are shown in the time domain of re-referencing and high pass filtering. **A.** Unfiltered EEG. **B.** Re-referencing by subtraction of spatial ensemble average. **C.** High pass spatial filter set at .1 cycles/cm. **D.** High pass temporal filter set at 4 Hz. Duration: 1 s. Amplitude: 100 microvolts.

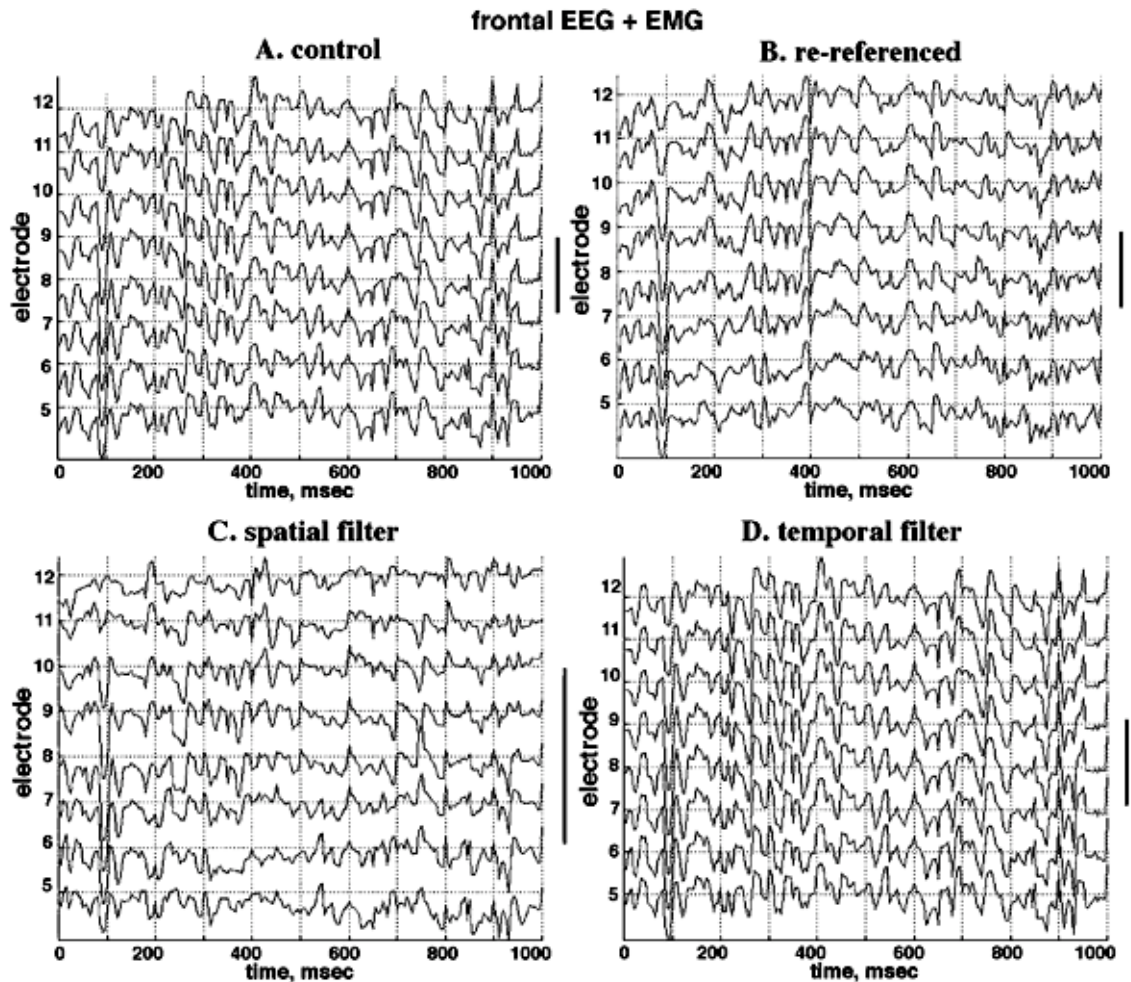


**Figure 12.** The effects on EEG + EMG (frontal, eyes closed) are shown of re-referencing and filtering. **A.** Unfiltered EEG + EMG. **B.** Re-referencing by subtraction of spatial ensemble average. **C.** High pass spatial filter set at .1 cycles/cm to remove Component 1 EMG. **D.** High pass temporal filter set at 4 Hz to remove Component 2 EMG. Duration: 1 s. Amplitude: 100 microvolts.

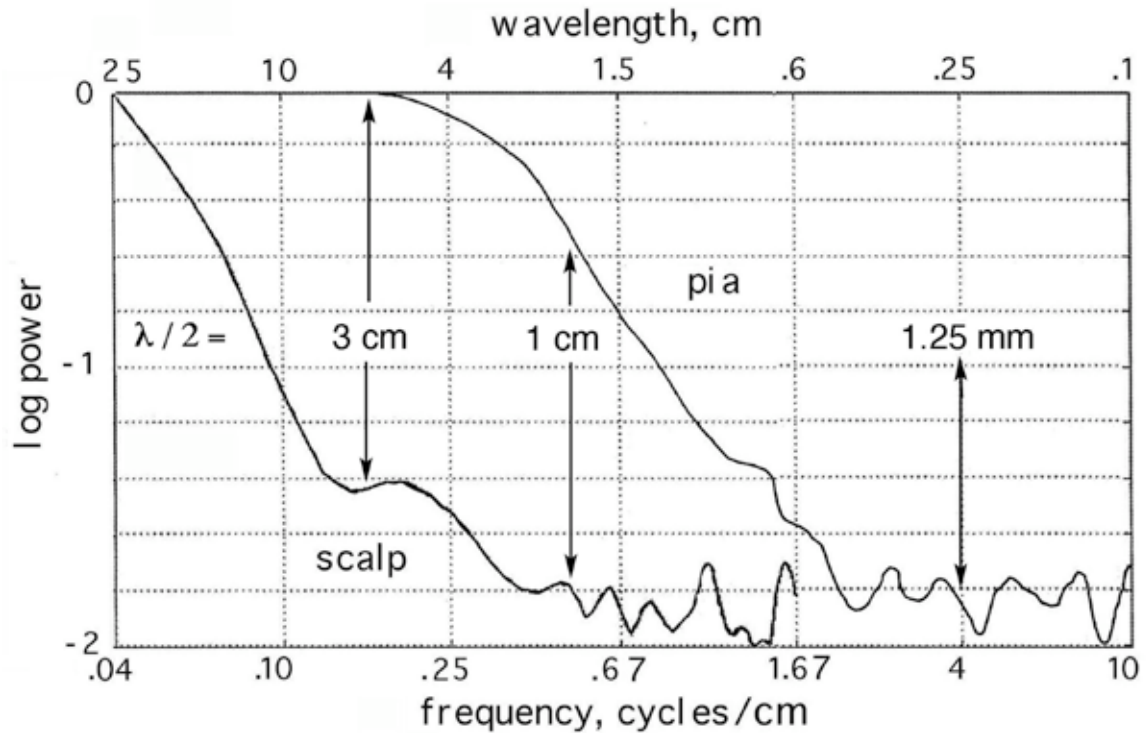


**Figure 13.** The  $PSD_x$  of the EEG from the pial surface of an awake neurosurgical patient with a  $1 \times 64$  electrode array having 0.5 mm spacing (from Freeman et al., 2000) is compared with the  $PSD_x$  from the scalp EEG of a normal volunteer with a  $1 \times 64$  array having 3 mm spacing. The ranges of the log-log spectra were normalized to 0 and -2 between the lowest and highest power. The frequency at which the spectral down-slope met a plateau in power was inferred to demarcate the boundary between signal and noise. The spatial sample rate should be minimally twice that frequency and preferably 3 to 5 times greater (Barlow, 1993). If the spectral peaks in the middle spatial range can be shown to have behavioral correlates, then by this criterion the optimal interval between scalp electrodes would be 5 to 8 mm. Such close spacing would also facilitate spatial filtering to reduce individual electrode noise.